VISUAL COARSENESS REPRESENTATION BY MEANS OF FUZZY SETS

J. Chamorro-Martínez, P. Martínez-Jiménez
Department of Computer Science and Artificial Intelligence
University of Granada
{jesus,pmartinez}@decsai.ugr.es

Abstract

In this paper, the texture feature ”coarseness” is modelled by means of fuzzy sets, relating representative coarseness measures (our reference set) with the human perception of this type of feature. In our study, a wide variety of measures have been analyzed, defining unidemsional and bidimensional fuzzy set for different combination of measures. The fineness human perception has been collected from polls filled by human subjects, performing an aggregation of their assessments by means of OWA operators. Using as reference set a combination of some measures, the membership function corresponding to the fuzzy set is modelled as the function which provides the best fit of the collected data.

Keywords: Image features, textural features, fuzzy texture, human perception, coarseness, fineness.

1 INTRODUCTION

It is usual for humans to describe visual textures according to some vague ”textural concepts” like *coarseness/fineness*, *orientation* or *regularity* [2, 17, 22]. From all of them, the *coarseness/fineness* is the most popular one, being common to associate the presence of fineness with the presence of texture (from this point of view, texture is defined as local variations against the idea of homogeneity). In this sense, a *fine* texture is considered as small texture primitives with big gray tone differences between neighbor primitives (e.g. the image in figure 1(A)), whereas a *coarse* texture corresponds to bigger primitives formed by several pixels (e.g. the image in figure 1(I)). By considering the importance of this textural concept, in this paper we will focus our study on the ”fineness” modelling (let us remark that ”coarseness” and ”fineness” are opposite but related textural concepts).

There are many measures in the literature that, given an image, capture the fineness (or coarseness) presence in the sense that the greater the value given by the measure, the greater the perception of texture [9]. However, there is no perceptual relationship between the value given by these measures and the degree in which the humans perceive the texture. Thus, given a certain value calculated by applying a measure to an image, there is not an immediate way to decide whether there is a fine texture, a coarse texture or something intermediate (i.e. there is not a textural interpretation).

The imprecision associated to these fineness measures suggests the use of representation models that incorporate the uncertainty. Nevertheless, the majority of the approaches that can be found in the literature are crisp proposals [5, 9, 18, 22] where uncertainty is not properly taken into account. To face this problem, fuzzy logic has been recently employed for representing the imprecision related to texture. However, in many of these approaches, fuzzy logic is usually applied just during the process but the output do not habitually model the imprecision (being often a crisp one). Examples of this fact are frequently found in the literature, like those approaches that use texture to perform image segmentation or classification on the basis of fuzzy clustering [8, 20, 23], fuzzy rules [6, 10, 16], etc.

Other interesting approaches emerge from the content-based image retrieval scope, where semantic data is managed by means of fuzzy sets [12, 13]. In these proposals, a mapping from low-level statistical features to high level textural concepts is performed by defining membership functions for each textural feature. However, given a feature, these membership functions are not obtained by considering the relationship between the computational feature and the human perception of texture, so the linguis-

[1]This work has been partially supported by the Andalusian Government under the TIC1570 and TIC249

tic labels related to these membership functions do not necessarily match what a human would expect.

In this paper we propose to solve this problem by representing the concept of fineness on the basis of fuzzy sets relating representative measures of the modelled texture (usually some statistic) with its human perception of fineness. In our analysis, a wide variety of measures have been considered, including classical statistical measures, frequency domain and fractal dimension measures, etc. Thus, this paper propose a group of fuzzy sets (defined on different measures) which model the textural fineness according to the human perception. The performance of each fuzzy set is analyzed and checked with the human assessments, proposing a subgroup of them as the most adequate for modelling fineness perception in texture images.

The rest of the paper is organized as follows. In section 2 we introduce our methodology to obtain the fuzzy sets that model the fineness textural concept. In section 3 we show the results of applying the models and the main conclusions and future work are summarized in section 4.

2 FUZZY MODELLING OF FINENESS

In this paper we propose to model the fineness perception as a fuzzy set defined on the domain of a given set of measures. For this purpose, two questions will be faced: (i) what reference set should be used for the fuzzy set, and (ii) how to obtain the related membership functions.

As reference set, a vector of fineness measures will be used. Concretely, we have analyzed the $K = 17$ measures indicated in the first column of table 1, that includes classical statistical measures well known in the literature, measures in the frequency domain, fractal dimension analysis, etc. All of them are automatically computed from the texture image. From now on, we will note $\mathcal{P} = \{P_1, \ldots, P_K\}$ the set of K measures of fineness analyzed in this paper, $F \subseteq \mathcal{P}$ a subset of $K' \leq K$ measures, and $\mathcal{T}_F$ the fuzzy set defined on the domain of F[1].

To obtain the membership function[2] of the fuzzy set $\mathcal{T}_F$, a functional relationship between the subset of measures F and the presence degree of fineness related to it will be learnt. To do it, we will use a set $\mathcal{I} = \{I_1, \ldots, I_N\}$ of N images that fully represent the different degrees of fineness. Thus, for each image $I_i \in \mathcal{I}$, we will obtain (a) a vector of measures $\mathbf{M}^i = [m^i_1, \ldots, m^i_{K'}]$, where m^i_k is a value for the measure $P_k \in \mathcal{P}$ applied to the image I_i, and (b) a human assessment of the fineness degree perceived, noted as v^i, which will be collected by means of a poll with human subjects (section 2.1). Once we have a multiset of valid pairs $\Psi_F = \{(\mathbf{M}^1, v^1), \ldots, (\mathbf{M}^N, v^N)\}$, we shall estimate the membership function by fitting a suitable function to the multiset of points Ψ (section 2.2).

Figure 1: Some examples of images with different degrees of fineness

2.1 ASSESSMENT COLLECTION

In this section, the way to obtain a vector $\Gamma = [v1, \ldots, v^N]$ of the assessments of the perception degree of fineness from the image set $\mathcal{I} = \{I_1, \ldots, I_N\}$ will be described. Thus, firstly the image set $\mathcal{I}$ will be selected. After that, a poll which allows to get assessments of the perception degree of fineness will be designed. These assessments will be obtained for each image in $\mathcal{I}$, so an aggregation of the different assessments will be performed.

[1] Given a set $\mathcal{P}$ of K measures, the fuzzy set $\mathcal{T}_F$ can be defined by using all the measures ($K' = K$) or a subset of them ($K' < K$)

[2] To simplify the notation, as it is usual in the scope of fuzzy sets, we will use the same notation $\mathcal{T}_F$ for the fuzzy set and for the membership function that defines it

2.1.1 The texture image set

A set $\mathcal{I} = \{I_1, \ldots, I_N\}$ of $N = 80$ images representative of the concept of *fineness* has been selected. Figure 1 shows some images extracted from the set $\mathcal{I}$. Such set has been selected satisfying the following properties:

1. It covers the different presence degrees of fineness.
2. The number of images for each presence degree is representative enough.
3. Each image shows, as far as possible, just one presence degree of fineness.

Due to the third property, each image can viewed as "homogeneous" respect to the fineness degree represented, i.e., if we select two random windows (with a dimension which does not "break" the original texture primitives and structure), the perceived fineness will be the same for each window (and also respect to the original image). In other words, we can see each image $I_i \in \mathcal{I}$ as a set of lower dimension images (windows) with the same fineness degree of the original one. For example, images of Figure 1 are 128×128 in size, but the perceived fineness is the same for windows of size 32×32; from this point of view, we can think in $I_i \in \mathcal{I}$ as an unique image of size 128×128 or as 9216 images of size 32×32 (all of them with the same degree of fineness).

As we explained in the introduction of this section, given an image $I_i \in \mathcal{I}$, we obtain a vector of measures $\mathbf{M}^i = [m_1^i, \ldots, m_{K'}^i]$, with m_k^i being the result of applying the measure $P_k \in \mathcal{P}$ to the image I_i. However, and thanks to the third property, we really can obtain a set of vectors associated to each image $I_i \in \mathcal{I}$ (one vector for each window). Let W be the number of windows considered for each image; from now on we will note as $\mathbf{M}_w^i = [m_1^{i,w}, \ldots, m_{K'}^{i,w}]$, with $w = 1, \ldots, W$, the vector of measures for the w-th window of the image I_i, with $m_k^{i,w}$ being the result of applying the measure $P_k \in \mathcal{P}$ to the w-th window of the image I_i. Therefore, the multiset of valid pairs $\Psi_F =$ will be given by $\Psi_F = \{(\mathbf{M}_w^i, v^i), i = 1, \ldots, N; w = 1, \ldots, W\}$.

2.1.2 The poll

Given the image set $\mathcal{I}$, the next step is to obtain assessments about the perception of fineness from a set of subjects. From now on we shall note as $\Theta^i = [o_1^i, \ldots, o_L^i]$ the vector of assessments obtained from L subjects for the image I_i. To get Θ^i, subjects will be asked to assign images to classes, so that each class has associated a perception degree of fineness.

In particular, 20 subjects have participated in the poll and 9 classes have been considered. The first nine images in figure 1 show the nine representative images for each class used in this poll. It should be noticed that the images are decreasingly ordered according to the presence degree of the fineness concept. The first class (Figure 1(A)) represents a presence degree of 1 while the ninth class (Figure 1(I)), represents a presence degree of 0. The rest of the classes (Figure 1(B)-(H)) represent degrees in the interval (0,1).

As result, a vector of 20 assessments $\Theta^i = [o_1^i, \ldots, o_{20}^i]$ is obtained for each image $I_i \in \mathcal{I}$. The degree o_j^i associated to the assessment given by the subject S_j to the image I_i is computed as $o_j^i = (9 - k) * 0.125$, where $k \in \{1, \ldots, 9\}$ is the index of the class C_k to which the image is assigned by the subject.

2.1.3 Assessment aggregation

Our aim at this point is to obtain, for each image in the set $\mathcal{I}$, one assessment v^i that summarizes the assessments Θ^i given by the different subjects about the presence degree of fineness.

To aggregate opinions we have used an OWA operator guided by a quantifier [25]. Concretely, the quantifier "the most" has been employed, which allows to represent the opinion of the majority of the polled subjects. This quantifier is defined as

$$Q(r) = \begin{cases} 0 & \text{if } r < a, \\ \frac{r-a}{b-a} & \text{if } a \leq r \leq b, \\ 1 & \text{if } r > b \end{cases} \quad (1)$$

with $r \in [0, 1]$, $a = 0.3$ and $b = 0.8$. Once the quantifier Q has been chosen, the weighting vector of the OWA operator can be obtained following Yager [25] as $w_j = Q(j/L) - Q((j-1)/L), j = 1, 2, ..., L$. According to this, for each image $I_i \in \mathcal{I}$, the vector Θ^i obtained from L subjects will be aggregated into one assessment v^i as follows:

$$v^i = w_1 \hat{o}_1^i + w_2 \hat{o}_2^i + ... + w_L \hat{o}_L^i \quad (2)$$

where $[\hat{o}_1^i, \ldots, \hat{o}_L^i]$ is a vector obtained by ranking in non-increasing order the values of the vector Θ^i.

2.2 FITTING THE MEMBERSHIP FUNCTION

At this point, the aim is to obtain, for a given subset of measures $F \subseteq \mathcal{P}$, the corresponding membership function $\mathcal{T}_F$. It is defined on a vector of K' real measures, i.e.,

$$\mathcal{T}_F : \mathbb{R}^{K'} \rightarrow [0, 1] \quad (3)$$

with K' being the cardinality of F. Since we are searching for a function which associates the measure vectors ($\mathbf{M}_w^i$) and the human assessments of fineness (v^i), we propose to estimate $\mathcal{T}_F$ by fitting a suitable curve to the multiset of points $\Psi_F = \{(\mathbf{M}_w^i, v^i), i = 1, \ldots, N; w = 1, \ldots, W\}$.

The values of the measures can be affected by some factors independent of the fineness (brightness, contrast, noise), which typically causes outliers in the fitting points. For this reason, in our approach the membership function is calculated by means of a Robust Fitting of the multiset Ψ_F (this fitting could be done according to some constraints, for example, to obtain a monotonic function). The robust fitting methods avoid that these outliers move the solution far from the true fit, as it happens in least squares. For this purpose we propose one of the most used techniques in computer vision: M-estimation.

M-estimators are a generalization of the traditional maximum likelihood estimation and, therefore, of the least squares fitting. If we consider a function $\mathcal{T}_F$ defined by D parameters $p_1, \ldots, p_D$, these parameters will be obtained as follows:

$$\underset{p_1,\ldots,p_D}{\operatorname{argmin}} \sum_{i=1}^{N} \rho\left(\mathbf{r}_w^i\right) \tag{4}$$

where $\mathbf{r}_w^i$ are the fitting residuals defined as

$$\mathbf{r}_w^i = v^i - \mathcal{T}_F(\mathbf{M}_w^i; p_1 \ldots p_D) \tag{5}$$

and the function ρ gives the contribution of each residual in the model, whose objective is to reduce the effect of outliers. This function ρ should have the following properties:

- ρ should be a symmetric, positive-definite function.
- ρ should have a unique minimum at zero (when the residual is zero).
- ρ should be derivable.

The minimization problem is solved by finding the parameters $p_1, \ldots, p_D$ which are the solution of the following system of D equations:

$$\sum_{i=1}^{N} \frac{\partial \rho\left(\mathbf{r}_w^i\right)}{\partial \mathbf{r}_w^i} \frac{\partial \mathbf{r}_w^i}{\partial p_j} = 0 \qquad j = 1, \ldots, D \tag{6}$$

Instead of solving directly this problem, we define a weight function

$$\omega(x) = \frac{\partial \rho(x)/\partial x}{x} \tag{7}$$

and then, Equation 6 becomes

$$\sum_{i=1}^{N} \omega\left(\mathbf{r}_w^i\right) \mathbf{r}_w^i \frac{\partial \mathbf{r}_w^i}{\partial p_j} = 0 \qquad j = 1, \ldots, D \tag{8}$$

which is a weighted least-squares problem. The weights, however, depend on the residuals, the residuals depend on the estimated coefficients, and the estimated coefficients depend on the weights. Therefore, an iterative solution (called iteratively reweighted least-squares, IRLS) is required. This process alternates steps of calculating the weights using the current estimated coefficients and solving Equation 8 to estimate the new coefficients with the weights fixed.

The function ρ is chosen so that the weights assigned to possible outliers become smaller in each iteration. We have taken one of the most commonly used functions in literature, that achieves a robust outlier rejection: the Tukey's biweight function [3]. The definition of the objective function $\rho(\mathbf{r}_w^i)$ and the weight function $\omega(\mathbf{r}_w^i)$ is:

$$\rho(\mathbf{r}_w^i) = \begin{cases} \frac{k^2}{6}\left[1 - \left(1 - \left(\frac{\mathbf{r}_w^i}{k}\right)^2\right)^3\right] & \text{if } \left|\mathbf{r}_w^i\right| \le k \\ \frac{k^2}{6} & \text{if } \left|\mathbf{r}_w^i\right| > k \end{cases} \tag{9}$$

$$\omega(\mathbf{r}_w^i) = \begin{cases} \left(1 - \left(\frac{\mathbf{r}_w^i}{k}\right)^2\right)^2 & \text{if } \left|\mathbf{r}_w^i\right| \le k \\ 0 & \text{if } \left|\mathbf{r}_w^i\right| > k \end{cases} \tag{10}$$

where k is a parameter called the *tuning constant* and it is defined as

$$k = 4.685\sigma \qquad \text{with } \sigma = \frac{median\left|\mathbf{r}_w^i - \mu_r\right|}{0.6745} \tag{11}$$

This parameter k must be recalculated in each iteration.

It should be noticed that there is an error related to the fitting (the mean of the absolute difference between the data points and the curve). This error can also be viewed as a goodness measure of the measures used in F; according to this, different subsets of measures could be analyzed, selecting the one with the lowest error.

For selecting the K' measures which compounds the subset F, we can consider 2^K possible combinations. These possible combinations include from a vector comprised of K items to vectors with only one item. In this paper, the cases of $K' = 1$ and $K' = 2$ will be considered. The first case ($K' = 1$) will allow to perform a study of each measure separately and to compare its goodness to model the *fineness*; the second one ($K' = 2$) will allow to combine measures in order to improve the individual ones. For higher dimensions ($K' \ge 3$) the Robust Fitting is too complex, so new methods for finding $\mathcal{T}_F$ need to be considered (for example, some kind of heuristic approaches). These cases will be considered in future works.

Table 1: Fitting errors related to each measure and parameter values for the two measures with least error

Measure	Error
Correlation [9]	0.1466
Amadasun [2]	0.1515
Abbadeni [1]	0.1880
Fractal dim. (FD) [15]	0.1891
Tamura [22]	0.1994
Edge density (ED) [4]	0.2044
DGD [11]	0.2120
Local Homogeneity [9]	0.2156
Short Run Emphasis [7]	0.2211
SNE [21]	0.2365
Weszka [24]	0.2383
Newsam [14]	WSD
Entropy [9]	WSD
Uniformity[9]	WSD
FMPS [26]	WSD
Variance[9]	NR
Contrast [9]	NR

Parameters for Correlation	
a_3	-1.83828
a_2	1.23377
a_1	-1.20788
a_0	1.03395
α	0.76851
β	0.02893

Parameters for Amadasun	
a_3	-0.00006
a_2	0.00556
a_1	-0.17053
a_0	1.57472
α	16.5285
β	3.82800

To define $\mathcal{T}_F$, the following considerations will be taked into account:

- $\mathcal{T}_F$ should be a monotonic function
- The values $\mathcal{T}_F(x) = 0$ and $\mathcal{T}_F(x) = 1$ should be achieved from a certain value

2.2.1 Unidimensional fitting

Regarding the above properties, in the case of $K' = 1$ we propose to define $\mathcal{T}_k$ as a function

$$\mathcal{T}_k : \mathbb{R} \rightarrow [0, 1] \tag{12}$$

of the form[3]

$$\mathcal{T}_k(x; a_n \dots a_0, \alpha, \beta) = \begin{cases} 0 & x < \alpha, \\ poly^n(x; a_n \dots a_0) & \alpha \leq x \leq \beta, \\ 1 & x > \beta \end{cases} \tag{13}$$

with $poly^n(x; a_n \dots a_0)$ being a polynomial function

$$poly^n(x; a_n \dots a_0) = a_n x^n + \dots + a_1 x^1 + a_0 \tag{14}$$

In our proposal, the parameters $a_n \dots a_0$, α and β of the function $\mathcal{T}_k$ are calculated by carrying out a Robust Fitting on Ψ_k taking into account the restriction of obtaining a monotonic function and considering n=1,2,3 (i.e. linear, quadratic and cubic functions) to define the polynomial function. Table 1 shows for each measure $P_k \in \mathcal{P}$ the least fitting error obtained. Note that this value can be viewed as a goodness measure of the ability of the measure to represent the perception of fineness.

Table 1 has been sorted in increasing order of the errors. The parameter values of the two measures with the lowest error (Correlation and Amadasun) are also shown in Table 1. It should be noticed that we haven't carried out the fitting with six of the measures. Four of them (marked with WSD) are rejected because their values are affected by the window size, ie., they are window size dependent. The other two (marked with NR) produce a diffuse cloud of points Ψ_F which implies that these measures are not providing a representative information about the perception of fineness.

2.2.2 Bidimensional fitting

In the case of $K' = 2$ we define $\mathcal{T}_k$ as a function

$$\mathcal{T}_k : \mathbb{R}^2 \rightarrow [0, 1] \tag{15}$$

of the form

$$\mathcal{T}_k(x, y; a_{(n!+n)} \dots a_0) = \mathcal{T}_k(x, y; coef) =$$

$$= \begin{cases} 0 & poly2^n(x, y; coef) < 0, \\ poly2^n(x, y; coef) & 0 < poly2^n(x, y; coef) < 1, \\ 1 & poly2^n(x, y; coef) > 1 \end{cases} \tag{16}$$

with $poly2^n(x, y; coef)$ being a polynomial function of two variables

$$poly2^n(x, y; a_{(n!+n)} \dots a_0) = \sum_{i=0}^{n} \sum_{j=0}^{i} a_{(i!+j)} x^j y^{i-j} =$$

$$= a_{(n!+n)} x^n + a_{(n!+n-1)} x^{n-1} y^1 + \dots + a_2 x^1 + a_1 y^1 + a_0 \tag{17}$$

Like in the previous case, the parameters $a_{(n!+n)} \dots a_0$ of the function $\mathcal{T}_k$ are calculated by carrying out a Robust Estimation considering n=1,2,3 to define the polynomial function,but in this case the fitting points are located in a tridimensional space and the polynomial function has two variables. The measures are taken in pairs by combining only the first six measures in Table 1.

Table 2 shows the least fitting error obtained for each pair of measures. It can be noticed that the first pair of measures (FD + Amadasun) obtains a fitting error much smaller than the others, but moreover it is much smaller than the fitting error of each measure separately. This implies that it provides the most representative information about the perception of fineness. The parameter values of this pair of measures appear in Table 2.

[3] Note that this function is defined for measures that increase according to the perception of fineness but for those that decreases, the function needs to be changed appropriately

Table 2: Fitting errors related to each pair of measures and parameter values for the pair with least error

Measure x	Measure y	Error
FD	Amadasun	0.1095
Correlation	ED	0.1332
Correlation	Tamura	0.1339
Amadasun	Correlation	0.1354
Abbadeni	Tamura	0.1373
Amadasun	ED	0.1431
Correlation	Abbadeni	0.1433
Abbadeni	Amadasun	0.1444
Correlation	FD	0.1455
Abbadeni	FD	0.1475
Tamura	Amadasun	0.1529
FD	Tamura	0.1634
ED	Tamura	0.1636
ED	FD	0.1764
Abbadeni	ED	0.1799

Parameters for FD+Amadasun	
a_9	1.11686
a_8	-0.00076
a_7	0.00000
a_6	-0.00853
a_5	-11.3885
a_4	0.06165
a_3	0.22887
a_2	36.8053
a_1	-1.26158
a_0	-34.7570

3 Results

In this section, the membership function $\mathcal{T}_k$ with least fitting error (obtained for the pair of measures FD+Amadasun and defined by the parameter values shown in Table 2) will be applied in order to analyze the performance of the proposed model. For this purpose, some experiments using images with different associated fineness presence degrees will be performed, analyzing the goodness of the fuzzy set to represent the perception of fineness. Moreover, these results will be compared with those obtained by using directly the measure values in order to verify the improvements introduced by the model.

Let's consider Figure 2(A) corresponding to a mosaic made by several images, each one with a different increasing perception degree of fineness. The perception degree of fineness for each subimage has been calculated using the proposed model and the results are shown in Figure 2(B) where a white grey level means maximum perception of fineness, while a black one corresponds to no perception of fineness. The numeric values are also shown on each subimage: v is the value of the human assessment and f is the computed degree. It can be noticed that our model captures the evolution of the perception degrees of fineness.

Figure 2(C) shows a mapping from the original image to its "fineness" membership degree using the proposed model. For each pixel in the original image, a centered window of size 32×32 has been analyzed and its fineness membership degree has been calculated. Thus, Figure 2(C) represents the degree in which the human perceives the texture, with a white grey level meaning maximum perception of fineness, and a black one meaning no perception of fineness (i.e., maximum perception of coarseness). The histogram of this image is shown beside it. We can see four clearly differ-

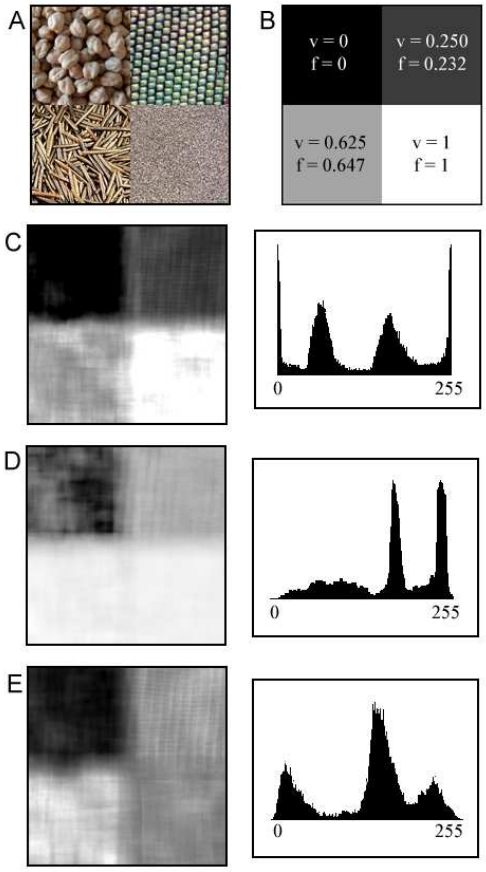

Figure 2: Results for a mosaic image. (A) Original mosaic image (B) Degree of fineness obtained with the proposed model for the pair of measures FD+Amadasun (C)(D)(E) Fineness membership degree of each pixel obtained with the proposed model and with the individual measures Amadasun and FD, respectively, and histograms of these images

enced peaks, corresponding to the four different fineness degrees in the image.

Figures 2(D) and 2(E) show a mapping from the original image using the Amadasun and FD measures directly, without any model. In this case the grey level of each pixel represents the obtained measure value instead of the perception degree of fineness so these images don't provide as much perceptual information as Figure 2(C). Furthermore, their histograms show that the four peaks can't be obtained with both measures separately.

Figure 3 presents an example where the proposed fuzzy sets have been employed for pattern recognition. In this case, the figure shows a microscopy image (Figure 3(A)) corresponding to the microstructure of a metal sample [19]. The lamellae indicates islands of eutectic, which are to be separated from the uniform light regions. The brightness values in regions of the original image are not distinct, so

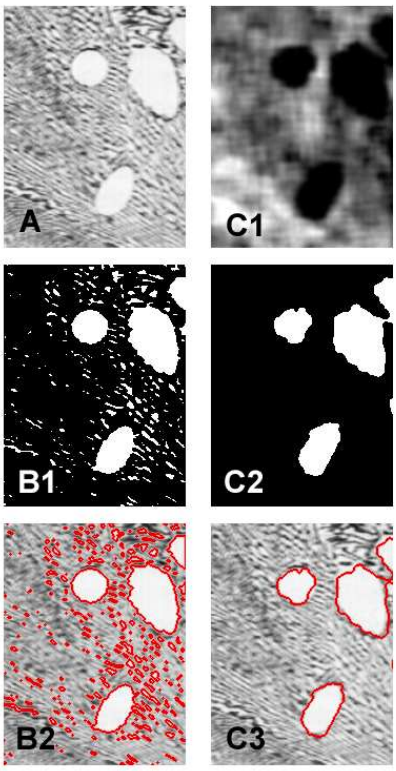

Figure 3: Example of pattern recognition using the proposed model (A) Original image (B1) Binary image obtained by thresholding the original image (B2) Region outlines of B1 superimposed on original image (C1) Fineness membership degrees obtained with our model from the original image (C2) Binary image obtained by thresholding C1 (C3) Region outlines of C2 superimposed on original image

texture information is needed for extracting the uniform areas. This fact is showed in Figure 3(B1,B2), where a thersholding on the original image is displayed (homogeneous regions cannot be separated from the textured ones as they "share" brightness values).

Figure 3(C1) shows a mapping from the original image to its "fineness" membership degree. In this case, we use a window of size 20×20. Thus, Figure 3(C1) represents the degree in which the human perceives the texture and it can be noticed that uniform regions correspond to areas with low degrees of fineness (i.e., high coarseness), so if only the pixels with fineness degree lower than 0.1 are selected (which it is equivalent to a coarseness degree upper than 0.9), the uniform light regions emerge with ease (Figure 3(C2,C3)).

4 Conclusions

In this paper, fuzzy sets for fineness perception have been defined on the domain of certain measures. The membership function associated to the fuzzy set has been learnt by finding the functional relationship between a certain measure (automatically computed over the image) and the presence degree of the textural concept. The measures have been chosen so that they collect information of the textural fineness under study whereas the presence degree has been obtained by performing a poll with humans and aggregating their assessments by means of OWA operators. Satisfactory performance has been found when using the different fuzzy sets with real images and the results show a high level of connection with the assessments given by subjects.

References

[1] N. Abbadeni, N. Ziou, and D.S. Wang. Autocovariance-based perceptual textural features corresponding to human visual perception. In *Proc. of 15th International Conference on Pattern Recognition*, volume 3, pages 901–904, 2000.

[2] M. Amadasun and R. King. Textural features corresponding to textural properties. *IEEE Transactions on Systems, Man and Cybernetics*, 19(5):1264–1274, 1989.

[3] A.E. Beaton and J.W. Tukey. The fitting of power series, meaning polynomials, illustrated on band-spectroscopic data. *Technometrics*, 16:147–185, 1974.

[4] J. Canny. A computational approach to edge detection. *IEEE Transactions on Pattern Analysis and Machine Intelligence*, 8(6):679–698, 1986.

[5] K.I. Chang, K.W. Bowyer, and M. Sivagurunath. Evaluation of texture segmentation algorithms. In *Proc. IEEE Computer Society Conference on Computer Vision and Pattern Recognition*, volume 57, pages 294–299, 2003.

[6] X. Dai and J. Maeda. Unsupervised segmentation of textured color images using fuzzy homogeneity decision. In *Proc. 4th International Symposium on Video/Image Processing and Multimedia Communications*, pages 75–78, 2002.

[7] M.M. Galloway. Texture analysis using gray level run lengths. *Computer Graphics and Image Processing*, 4:172–179, 1975.

[8] M. Hanmandlu, V. K. Madasu, and S. Vasikarla. A fuzzy approach to texture segmentation. In *Proc. International Conference on Information Technology:*

Coding and Computing, volume 1, pages 636–642, 2004.

[9] R.M. Haralick. Statistical and structural approaches to texture. *Proceedings IEEE*, 67(5):786–804, 1979.

[10] G. Karmakar, L. Dooley, and M. Murshed. Fuzzy rule for image segmentation incorporating texture features. In *Proc. of 2002 International Conference on Image Processing*, volume 1, pages I–797–I–800, 22-25 Sept. 2002.

[11] S.I. Kim, K.C. Choi, and D.S. Lee. Texture classification using run difference matrix. In *Proc. of IEEE 1991 Ultrasonics Symposium*, volume 2, pages 1097–1100, December 1991.

[12] S. Kulkarni and B. Verma. Fuzzy logic based texture queries for cbir. In *Proc. 5th International Conference on Computational Intelligence and Multimedia Applications*, pages 223–228, 2003.

[13] H.C. Lin, C.Y. Chiu, and S.N. Yang. Finding textures by textual descriptions, visual examples, and relevance feedbacks. *Pattern Recognition Letters*, 24(14):2255–2267, 2003.

[14] S.D. Newsam and C. Kammath. Retrieval using texture features in high resolution multi-spectral satellite imagery. In *Data Mining and Knowledge Discovery: Theory, Tools, and Technology VI, SPIE Defense and Security*, April 2004.

[15] S. Peleg, J. Naor, R. Hartley, and D. Avnir. Multiple resolution texture analysis and classification. *IEEE Transactions on Pattern Analysis and Machine Intelligence*, (4):518–523, 1984.

[16] M. Potrebić. Iterative fuzzy rule base technique for image segmentation. In *Proc. of 7th seminar on Neural Network Applications in Elecrical Engineering*, pages 221–224, 23-25 Sept. 2004.

[17] A.R. Rao and G.L. Lohse. Identifying high level features of texture perception. *Graphical Models and Image Processing*, 55(3):218–233, 1993.

[18] Todd R. Reed and J.M. Hans Du Buf. A review of recent texture segmentation and feature extraction techniques. *CVGIP: Image Understanding*, 57(3):359–372, 1993.

[19] J.C. Russ. *The Image Processing Handbook*. CRC Press and IEEE Press, third edition, 1999.

[20] A. Shackelford. A hierachical fuzzy classification approach for high-resolution multispectral data over urban areas. *IEEE Transactions on Geoscience and Remote Sensing*, 41(9):1920–1932, 2003.

[21] C. Sun and W.G. Wee. Neighboring gray level dependence matrix for texture classification. *Computer Vision, Graphics and Image Processing*, 23:341–352, 1983.

[22] H. Tamura, S. Mori, and T. Yamawaki. Textural features corresponding to visual perception. *IEEE Trans. on Systems, Man and Cybernetics*, 8:460–473, 1978.

[23] C.B. Wang, H.B. Wang, and Q.B. Mei. Texture segmentation based on an adaptively fuzzy clustering neural network. In *Proc. of 2004 International Conference on Machine Learning and Cybernetics*, volume 2, pages 1173–1176, 2004.

[24] J.S. Weszka, C.R. Dyer, and A. Rosenfeld. A comparative study of texture measures for terrain classification. *IEEE Trans. on SMC*, 6:269–285, 1976.

[25] R.R. Yager. On ordered weighted averaging aggregation operators in multicriteria decisionmaking. *IEEE Trans. on SMC*, 18(1):183–190, 1988.

[26] H. Yoshida, D.D. Casalino, B. Keserci, A. Coskun, O. Ozturk, and A. Savranlar. Wavelet-packet-based texture analysis for differentiation between benign and malignant liver tumours in ultrasound images. *Physics in Medicine and Biology*, 48:3735–3753, 2003.